International Journal of Biological Macromolecules 322 (2025) 146912

Contents lists available at ScienceDirect

International Journal of Biological Macromolecules

journal homepage: www.elsevier.com/locate/ijbiomac

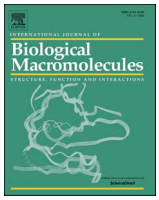

Peroxidase-laccase dual enzymatic activities of bovine serum albumin-copper hybrid nanoflowers for detecting ascorbic acid and degrading phenolic dyes

Xuan Ai Le [1], Thinh Viet Dang [1], Moon Il Kim [*]

Department of BioNano Technology, Gachon University, 1342 Seongnamdae-ro, Sujeong-gu, Seongnam, Gyeonggi 13120, Republic of Korea

ARTICLE INFO

Keywords:
Hybrid nanoflowers
Peroxidase mimic
Laccase mimic
Ascorbic acid detection
Phenolic dye degradation

ABSTRACT

Nanozymes have emerged as robust and cost-effective alternatives to natural enzymes; however, systems capable of mimicking multiple enzymatic activities remain limited. Here, we found that bovine serum albumin-copper hybrid nanoflowers (BSA-Cu NFs) exhibit unique dual enzymatic activities of peroxidase and laccase, which can be utilized for detecting ascorbic acid and degrading phenolic dyes, respectively. Among various metals including Cu, Mn, Zn, Fe, Co, and Ca, BSA-Cu NFs showed the most defined flower-like morphology presumably because Cu^{2+} ions exhibit a remarkable coordination ability toward the amine and amide groups of BSA. Importantly, among the diverse metal-incorporated NFs, BSA-Cu NFs exhibited the highest peroxidase-like activity to oxidize 3,3′,5,5′-tetramethylbenzidine (TMB) in the presence of hydrogen peroxide and laccase-like activity to oxidize epinephrine. Leveraging their peroxidase-like activity, BSA-Cu NFs enabled colorimetric detection of ascorbic acid via TMB reduction, achieving a detection limit of 0.15 μM (linear range: 1–60 μM), with successful validation in human serum. Their laccase-like activity facilitated rapid degradation of phenolic dyes such as crystal violet, neutral red, and rhodamine B, outperforming natural laccase. Notably, BSA-Cu NFs retained high catalytic activity across broad pH and temperature ranges and exhibited excellent stability and reusability. These results highlight the potential of self-assembled BSA-Cu NFs as a multifunctional nanozyme platform for both diagnostic and environmental applications.

1. Introduction

Ascorbic acid (vitamin C) plays a crucial role in maintaining human health, functioning as both a potent antioxidant and an essential cofactor in biochemical processes such as collagen biosynthesis, immune modulation, and iron metabolism [1]. Its accurate quantification is of high clinical and industrial relevance, as imbalances—either deficiency or excess—are associated with conditions ranging from scurvy and immune dysfunction to renal complications and oxidative stress-related pathologies [2]. While conventional detection techniques offer high sensitivity, they often rely on sophisticated instruments and labor-intensive procedures, limiting their use in resource-constrained or point-of-care settings. Parallel to this, environmental pollution from phenolic dyes—frequently discharged by textile, paper, and leather manufacturing—has emerged as a critical concern due to their persistence, acute toxicity, and carcinogenic potential [3]. Existing remediation strategies, including adsorption and oxidative degradation, suffer from limited efficacy and may introduce secondary contaminants. These challenges highlight the urgent need for innovative sensing and remediation platforms that are not only effective and economical but also environmentally benign.

Remarkable catalytic specificity and efficiency of natural enzymes have made them indispensable in numerous biotechnological applications; however, their inherent limitations, including poor operational stability, high production costs, and structural fragility, have constrained their real implementation [4,5]. Nanozymes, which are engineered nanomaterials with enzyme-mimicking properties, have emerged as promising alternatives that combine the catalytic capabilities of natural enzymes with enhanced stability, cost-effectiveness, and reusability [6,7]. Recent advancements in nanozyme research have yielded materials that can mimic the activities of various oxidoreductases, including peroxidase [8], oxidase [9], catalase [10], superoxide

* Corresponding author.
E-mail address: moonil@gachon.ac.kr (M.I. Kim).
[1] These authors contributed equally to this work.

https://doi.org/10.1016/j.ijbiomac.2025.146912
Received 2 June 2025; Received in revised form 4 August 2025; Accepted 13 August 2025
Available online 14 August 2025

dismutase [11], and laccase [12–14]. Building on these advances, nanozymes can be effectively employed in a wide range of practical applications, particularly in scenarios where traditional enzyme-based systems encounter significant limitations. However, most reported nanozymes are limited to mimicking a single enzymatic activity, which may constrain their functionality in multi-step or synergistic catalytic processes. Therefore, it is noteworthy to develop nanozymes with multiple enzyme-like activities, thereby expanding their applications beyond single-function. These multi-catalytic nanozymes have demonstrated distinct utility in the applications requiring synergistic reactions or cascade reactions, which span biosensing, environmental remediation, and therapeutic interventions [15–17].

Organic-inorganic hybrid nanoflowers (NFs), characterized by their distinctive flower-shaped hierarchical nanostructured morphology and high surface-to-volume ratio, have garnered significant attention as protein immobilization platforms [18,19]. Conventional enzyme immobilization strategies, such as physical absorption, covalent bonding, or entrapment with matrices like metal organic frameworks, covalent organic frameworks, polymers, gels, or carbon-based materials, often involve complex preparation steps, use of harsh chemicals, or suffer from drawbacks such as enzyme leaching and reduced activity [20]. In contrast, such hybrid NFs are formed through coordination between metal ions and amine/amide functional groups present in biomolecules, including proteins, resulting in flower-like assemblies that effectively entrap organic components within their three-dimensional frameworks under mild conditions without harmful solvents or cross-linking agents [21,22]. This architectural arrangement not only protects the encapsulated biomolecules from denaturation but also enhances their catalytic performance through microenvironmental optimization and substrate channeling effects [23]. In previous studies, natural enzymes, such as horseradish peroxidase, glucose oxidase, and laccase, have been predominantly incorporated into hybrid NFs to preserve or amplify their native activities [24–28]. In contrast, the potential of NFs to confer enzyme-mimicking properties remains largely unexplored. Furthermore, existing research on NF-type nanozymes has primarily centered on mimicking single enzyme activity, majorly that of peroxidase [22]. Therefore, developing advanced NF-type nanozymes that retain broad or multiple enzyme-like activities is crucial to widen their utility and range of applications.

Recent research has increasingly explored peroxidase- and laccase-mimicking nanozymes, including hybrid NFs, for applications in biomolecular sensing, such as ascorbic acid detection, and the degradation of synthetic dyes. These nanozymes are particularly attractive due to their high catalytic efficiency, robustness under diverse environmental conditions, and potential for reuse. For examples, amino acid–metal phosphate hybrid NFs have demonstrated peroxidase-like activity, enabling the sensitive detection of ascorbic acid [29]. Likewise, polyacrylonitrile–copper oxide hybrid NFs with strong peroxidase-mimetic properties have been utilized for the detection of H_2O_2 and ascorbic acid [30]. Laccase-mimicking nanozymes have also shown promise for environmental applications; in our previous study, Mn—Cu hybrid NFs exhibiting laccase-like activity effectively degraded phenolic dyes [31]. Despite these advances, multifunctional nanozyme platforms capable of exhibiting dual enzyme-mimicking activities and addressing a broad range of analytical and environmental targets remain relatively scarce. This gap underscores the need for continued innovation in the design of versatile and efficient nanozyme systems.

In this study, we developed bovine serum albumin-copper hybrid NFs (BSA-Cu NFs) that exhibit robust dual enzymatic activities comprising both peroxidase-like and laccase-like functionalities. Through systematic screening of various metal ions (Cu, Mn, Zn, Fe, Co, and Ca) as inorganic components, we demonstrate that Cu-incorporated NFs possess superior morphological characteristics and dual-enzymatic performance, which can be attributed to the exceptional coordination capacity of Cu^{2+} ions with the amine/amide groups of BSA. The synthesized BSA-Cu NFs exhibited remarkable catalytic parameters (K_m, V_{max}, and k_{cat}) that are comparable to or even surpass those of their natural enzyme counterparts and previously reported nanozymes while maintaining excellent stability across broad pH and temperature ranges. Leveraging these dual enzymatic capabilities, we employed BSA-Cu NFs for two distinct applications: (1) the colorimetric detection of ascorbic acid based on its antioxidant effect to induce the reduction of oxidized blue 3,3′,5,5′-tetramethylbenzidine (TMB) to colorless TMB and (2) the efficient degradation of phenolic dyes through laccase-like catalytic action, demonstrating the superior applicability of the NFs for dual purposes (Fig. 1). This dual-functional nanozyme system offers the advantages of facile synthesis, high catalytic efficiency for both enzyme-mimicking activities, and operational stability, although further optimization may be needed to balance the two functionalities.

2. Experimental section

2.1. Materials

Bovine serum albumin (BSA), copper(II) sulfate pentahydrate, manganese(II) sulfate monohydrate, zinc chloride, iron(II) sulfate heptahydrate, cobalt(II) sulfate heptahydrate, calcium chloride anhydrous, phosphate buffered saline (PBS), peroxidase from horseradish (HRP), laccase from *Trametes versicolor*, 2,2′-azino-bis(3-ethylbenzothiazoline-6-sulfonic acid) diammonium salt (ABTS), 3,3′,5,5′-tetramethylbenzidine (TMB), epinephrine, hydrogen peroxide (H_2O_2), L-ascorbic acid, crystal violet (CV), neutral red (NR), and rhodamine B (RB) were purchased from Sigma-Aldrich (Milwaukee, WI). All chemicals were of analytical grade or higher and were used as received without further purification, and the solutions were prepared with deionized water purified by a Milli-Q Purification System (Millipore, Darmstadt, Germany).

2.2. Synthesis and characterization of BSA-metal hybrid NFs

Hybrid NFs comprising BSA and various metal components, including Cu, Mn, Zn, Fe, Co, and Ca, were synthesized using a modified precipitation method [32]. Stock solutions of metal cations ($CuSO_4$, $MnSO_4$, $ZnCl_2$, $FeSO_4$, $CoSO_4$, and $CaCl_2$; 120 mM each) were individually prepared in deionized water. To synthesize the NFs, 60 μL of each solution was added to 9 mL of phosphate buffered saline (PBS, 10 mM, pH 7.4) containing 0.1 mg/mL BSA. The mixtures were left at room temperature (RT) for 3 days to allow self-assembly. The resulting precipitates were collected by centrifugation (10,000 ×*g*, 10 min) and washed thrice with deionized water to remove unreacted components. As control samples, metal phosphate precipitates ($Cu_3(PO_4)_2$, $Mn_3(PO_4)_2$, $Zn_3(PO_4)_2$, $Fe_3(PO_4)_2$, $Co_3(PO_4)_2$, $Ca_3(PO_4)_2$) were synthesized by mixing the above stock solutions of metal cations in PBS without the addition of BSA, and the other procedures were the same as described above.

The resulting BSA-metal hybrid NFs were characterized by scanning electron microscopy (SEM) with an energy-dispersive spectrometer (EDS), X-ray diffraction (XRD), Fourier transform infrared spectroscopy (FTIR), X-ray photoelectron microscopy (XPS), nitrogen physisorption using the Brunauer–Emmett–Teller (BET) and Barrett–Joyner–Halenda (BJH) methods, and bicinchoninic (BCA) assay. The experimental details were described in the Supplementary Information.

2.3. Evaluation of peroxidase-laccase dual-enzymatic activities of BSA-Cu NFs

Peroxidase- and laccase-like activities of the synthesized NFs were evaluated using TMB oxidation with H_2O_2 and epinephrine oxidation, respectively. Steady-state kinetic assays were performed at RT in a 1.5 mL tube with BSA-Cu NFs (0.1 mg/mL) in sodium acetate (50 mM, pH 4) and MES buffer (50 mM, pH 8) to determine the kinetic parameters of peroxidase- and laccase-like activities, respectively. In the kinetic

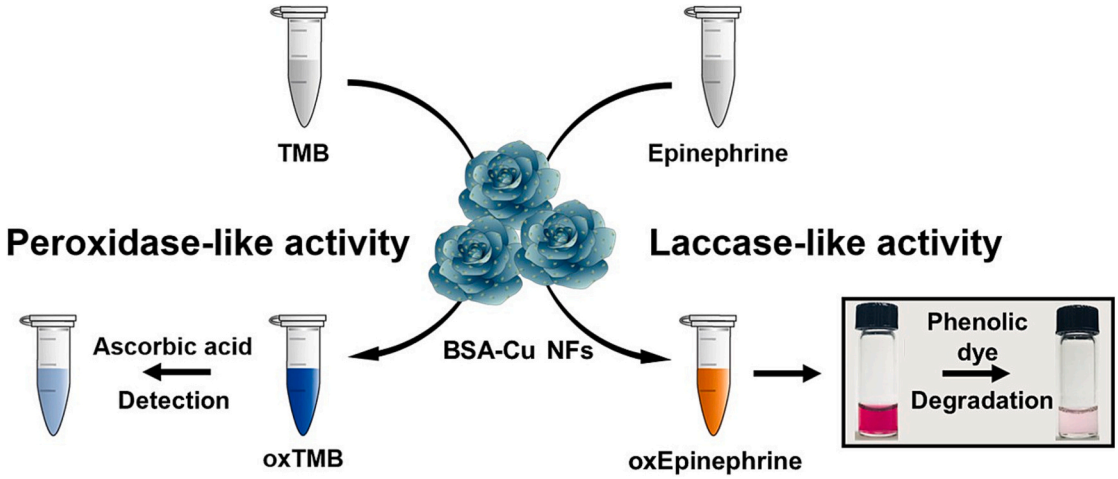

Fig. 1. Schematic illustration of the detection of ascorbic acid and degradation of phenolic dyes using the peroxidase-laccase dual enzymatic activities of BSA-Cu NFs.

assays, TMB and H_2O_2 were employed as substrates for peroxidase-like activity and epinephrine was used as a substrate for laccase-like activity. Details of the activity assays [33] were presented in the Supplementary Information.

2.4. Colorimetric detection of ascorbic acid based on the peroxidase-like activity of BSA-Cu NFs

Colorimetric detection of ascorbic acid was carried out based on its antioxidant action to induce the reduction of oxidized TMB, produced by the peroxidase-like activity of BSA-Cu NFs. The reaction mixture contained TMB (0.5 mM), BSA-Cu NFs (0.05 mg/mL), and H_2O_2 (10 mM) in sodium acetate buffer (100 μL, 50 mM, pH 4). After an initial incubation at RT for 15 min, the sample solution (100 μL) containing ascorbic acid was added into the blue-colored mixture, and after 1 min, the reduction in absorbance at 652 nm was recorded. The limit of detection (LOD) was calculated according to the following equation: LOD = 3S / K, where S is the standard deviation of the blank absorbance and K is the slope of the calibration plot. To assess the selectivity to detect ascorbic acid, possible interfering molecules at 10-fold higher concentration, such as carbohydrates (glucose, fructose, lactose), ions (Ca^{2+}, Na^{+}), amino acids (glycine, histidine), and protein (BSA), were added instead of ascorbic acid.

Human serum was diluted ten-fold to ensure that its ascorbic acid concentration fell within our linear detection range. To create spiked serum samples, a predefined amount (10, 15, 20, 30, and 40 μM) of ascorbic acid was added after measuring the original ascorbic acid concentration of human serum using an ascorbic acid assay kit (Sigma-Aldrich, Milwaukee, WI). Using the same methods described above, the ascorbic acid content of each spiked sample (100 μL) was determined.

2.5. Degradation of phenolic dyes based on the laccase-like activity of BSA-Cu NFs

Degradation of phenolic dyes, such as CV, NR, and RB, was performed using BSA-Cu NFs and natural laccase. Typically, BSA-Cu NFs and natural laccase (1 mg/mL each) were separately mixed in a solution (10 mL) containing CV (2.5 mg/L), NR (7.5 mg/L), and RB (1.5 mg/L). The mixtures were incubated in the dark at RT with constant stirring. The dye degradation efficiency was monitored by measuring the absorbance at specific wavelengths (CV: 590 nm, NR: 523 nm, and RB: 543 nm) using a microplate reader.

3. Results and discussion

3.1. Synthesis and characterization of hybrid NFs comprising BSA and diverse metals

To investigate the enzyme-mimicking functionalities of hybrid NFs, we synthesized the NFs by incorporating a standard protein BSA with various metal ions, including Cu, Mn, Zn, Fe, Co, and Ca. BSA was chosen as the template protein due to its wide availability, low cost, and excellent stability under various conditions [34]. Its abundant and multiple functional groups enable strong coordination with metal ions, facilitating the formation of stable hybrid nanostructures [35], which make it a practical and effective choice over other proteins. After self-assembly for three days at RT, the BSA-metal hybrid NFs were synthesized, which exhibited flower-like morphologies with an average size of 4–20 μm (Fig. 2). Among the tested NFs, BSA-Cu NFs showed the best flower-like hierarchical morphology with an average diameter of 5 μm and petal thickness of 64 nm, with the highest BSA encapsulation yield (Fig. S1a, Table S1). It is worth noting that the sample synthesized without BSA show only $Cu_3(PO_4)_2$ precipitates with no flower-like morphology (Fig. S1b). This is presumably due to the most efficient coordination between Cu^{2+} and the amine/amide moieties of BSA, as previously discussed [32,36]. BSA-Cu NFs were synthesized under mild conditions (10 mM PBS, pH 7.4 at RT) to preserve the structural integrity of BSA and minimize the risk of protein denaturation or conformational changes [37,38]. The synthesis medium remained at a stable pH (7.4) over 3 days (Fig. S1c), minimizing the risk of protein denaturation. Additionally, varying the PBS ionic concentration (10, 50, and 100 mM) had negligible impact on the flower-like morphology, confirming that

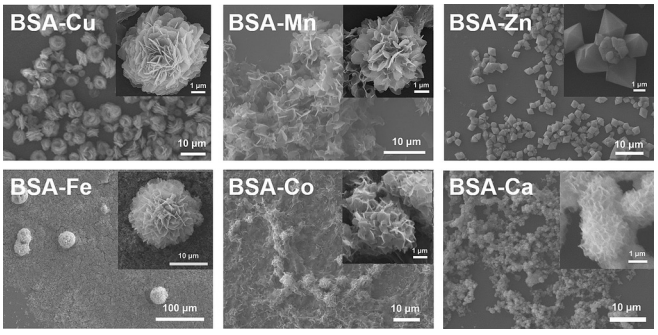

Fig. 2. SEM images of BSA-metal hybrid NFs. The insets show the NFs at high magnifications.

ionic strength did not adversely affect the formation or structure of BSA-Cu NFs (Fig. S1d).

The synthesized BSA-metal hybrid NFs were further characterized to clarify their structural features. EDS analysis confirmed the presence of the expected elements of N, O, and P, with the metals incorporated within the NFs (Fig. S2). The FTIR spectra of the NFs confirmed the presence of both BSA and metal phosphate components (Fig. S3). Particularly, characteristic peaks in the range of 1150–1050 cm^{-1} were

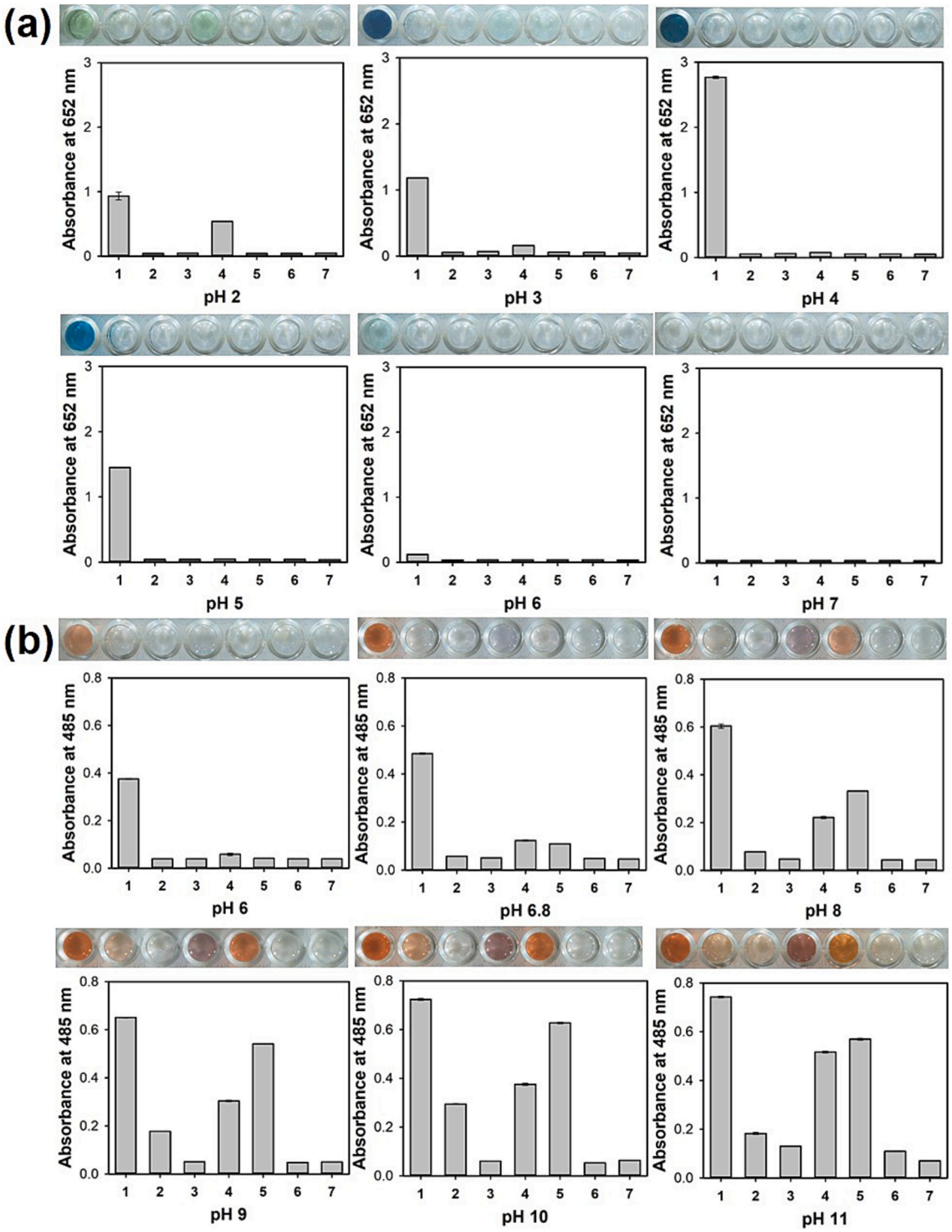

Fig. 3. Evaluation of the (a) peroxidase- and (b) laccase-like activities of BSA-metal hybrid NFs, by measuring the respective absorbances from the peroxidase-mediated oxidation of TMB in the presence of H_2O_2 and laccase-mediated oxidation of epinephrine, respectively, under various pH conditions. In each graph, real photographs after the reaction are shown. Numbers (1–7) in x-axis correspond to the following samples: BSA-Cu NFs, BSA-Mn NFs, BSA-Zn NFs, BSA-Fe NFs, BSA-Co NFs, BSA-Ca NFs, and a negative control, respectively. The peroxidase-like activity of different BSA-metal NFs was assessed by adding 100 μL of each NF solution (0.1 mg/mL) into 900 μL of sodium acetate buffer (50 mM, pH 2–7) containing 0.5 mM TMB and 10 mM H_2O_2. For laccase-like activity, 100 μL of each NF sample (0.1 mg/mL) was mixed with 900 μL of MES buffer (50 mM, pH 6–11) containing 0.1 mg/mL epinephrine. All reactions were incubated at RT for 15 min, after which the absorbance was recorded at 652 nm and 485 nm for peroxidase- and laccase-like activities, respectively.

assigned to the symmetric and asymmetric stretching vibrations of the PO_4^{3-} groups (P—O, and P═O), while the peak around 570 cm^{-1} corresponded to the bending vibration of metal-O bonds [39]. Additionally, peaks observed in the regions of 1700–1600 cm^{-1} and 1560–1500 cm^{-1} were attributed to amide I and amide II bands of BSA, respectively, indicating the presence of protein secondary structures [40]. XRD analysis confirmed the crystalline structure of the BSA-metal NFs, as evidenced by the sharp diffraction peaks corresponding to the respective metal phosphate phases (Fig. S4). As representative, the diffraction peaks of BSA-Cu NFs aligned well with those of standard $Cu_3(PO_4)_2$ (JCPDS No. 22-0548), indicating that the incorporation of BSA does not alter the crystallinity of the inorganic frameworks (Fig. S5). This preserved crystalline backbone is critical for ensuring the structural integrity and catalytic stability of the NFs. Nitrogen adsorption-desorption isotherms classified all the BSA-metal NFs as type IV with an H3 hysteresis loop (Fig. S6), indicating that the NFs exhibit nanoporous structures with a large surface area [41]. The specific surface area and pore size of the NFs ranged from 12.6 to 42.5 $m^2\ g^{-1}$ and 15.4 to 24.0 nm, respectively, which are comparable to those of reported hybrid NFs [42–44]. XPS was employed to assess the elemental composition and oxidation states of the NFs. The survey spectra of BSA-Cu NFs exhibited a distinct N 1s peak at ~400 eV, confirming the incorporation of BSA molecules, which was absent in the $Cu_3(PO_4)_2$ control (Fig. S7a). High-resolution Cu 2p spectra revealed the presence of mixed oxidation states (Cu^+ and Cu^{2+}), suggesting redox heterogeneity produced during synthesis (Fig. S7b) [45]. Additionally, the N 1s spectrum of BSA-Cu NFs showed peaks at 398.8, and 399.8 eV, corresponding to amine ligands, and Cu—N coordination, respectively (Fig. S7c) [46,47]. These characterizations confirmed the successful incorporation of metal ions and BSA within the NFs, while BSA-Cu NFs showed the best hierarchical flower-like morphology and BSA encapsulation efficiency.

3.2. Evaluation of the peroxidase-laccase dual-enzymatic activities of BSA-Cu NFs

Peroxidase-like activities of BSA-metal hybrid NFs were investigated by performing assay reactions under diverse pH environments using TMB as a chromogenic substrate with H_2O_2. The results showed that BSA-Cu NFs showed the highest peroxidase-like activity, producing the deepest blue color corresponding to the oxidized TMB under acidic and near-neutral pH conditions (pH 2–6) (Fig. 3a). BSA-Fe NFs could also oxidize TMB with H_2O_2 under acidic pH conditions (pH 2–3); however, the extent of their activity was not significant compared to that of BSA-Cu NFs. The other BSA-metal hybrid NFs did not show any meaningful activity under all tested pH conditions. In addition, the peroxidase-like activity of the BSA-Cu NFs was ~2.5-fold higher than that of $Cu_3(PO_4)_2$ precipitates, indicating that entrapped BSA is essential to enhance the activity presumably due to the much larger surface area due to the flower-like morphologies to facilitate substrate interactions (Fig. S8a) [36,50]. Control experiments with free Cu^{2+} and a non-structured Cu^{2+}/BSA mixture exhibited lower peroxidase-like activity compared to BSA-Cu NFs (Fig. S8b). The superior catalytic performance of BSA-Cu NFs is ascribed to their hierarchical nanoflower architecture, which offers an enlarged surface area with stable Cu active centers, enhanced substrate accessibility, and improved electron transfer dynamics. We then examined the production of hydroxyl radicals ($^{\bullet}OH$) during peroxidase-mediated H_2O_2 decomposition, using terephthalic acid (TA), a probe that reacts with $^{\bullet}OH$, to form highly fluorescent 2-hydroxy TA. The emission intensities proportionally increased as the concentration of BSA-Cu NFs increased, suggesting that the BSA-Cu NFs can produce $^{\bullet}OH$ from H_2O_2 due to their peroxidase-like activity (Fig. S8c). The underlying mechanism of peroxidase-like activity of BSA-Cu NFs is primarily driven by their copper-based catalytic centers, which mediate Fenton-like reactions (Fig. S8d).

To elucidate the peroxidase-mimicking behavior of BSA-Cu NFs, steady-state kinetic assays were conducted by alternately varying the concentration of either TMB or H_2O_2 while maintaining the other at a constant level. This approach enabled the generation of Michaelis–Menten and Lineweaver–Burk plots for both substrates (Fig. S9a), from which key kinetic parameters—K_m, V_{max}, and k_{cat}—were extracted. As summarized in Table S2, the K_m values for TMB and H_2O_2 were determined to be 0.593 and 0.936 mM, respectively. The affinity for TMB was comparable with that of natural horseradish peroxidase (HRP), while the markedly lower K_m for H_2O_2 indicated an enhanced substrate affinity compared to HRP and other nanozyme analogs. Furthermore, the k_{cat} value of BSA-Cu NFs ranked among the highest reported to date, underscoring their efficient catalytic performance. Specific activity (SA) of BSA-Cu NFs for peroxidase-like reaction was determined to be 8.73 U/mg, which is comparable to that of recently-reported peroxidase-mimicking nanozymes (Fig. S10a, b) [49,50]. This high catalytic efficiency is likely attributable to the densely populated active sites within the nanoflower architecture, where Cu ions are effectively coordinated with BSA molecules.

The laccase-like activities of BSA-metal hybrid NFs were assessed using epinephrine as a substrate. BSA-Cu NFs exhibited the highest activity under all the tested pH conditions (pH 6–11), although BSA—Mn, —Fe and —Co NFs also showed marginal activities (10–90 % to that of BSA-Cu NFs) under basic pH conditions (pH 8–11) (Fig. 3b). Compared to natural laccase, BSA-Cu NFs showed ~4-fold higher absorbance at 485 nm, similar to oxidized epinephrine (Fig. S11a). In addition, BSA-Cu NFs exhibited superior catalytic performance compared to control systems, including free Cu^{2+}, a physical mixture of Cu^{2+} and BSA, and $Cu_3(PO_4)_2$ precipitates, likely due to their well-defined flower-like nanostructure. The enhanced activity might be attributed to the entrapped Cu ions which mediate laccase action, similar to the four Cu elements present within the active site of natural laccase [51,52]. The laccase activity of the BSA-Cu NFs was further confirmed in another control experiment. While other oxidases produce H_2O_2, the BSA-Cu NFs directly converted oxygen into water without producing H_2O_2 (Fig. S11b) [53]. This was accomplished by incubating BSA-Cu NFs with 2,4-dichlorophenol (2,4-DP) for 30 min, followed by collection of the supernatant by centrifugation. HRP and the peroxidase substrate 2,2′-azino-bis(3-ethylbenzothiazoline-6-sulfonic acid) diammonium salt (ABTS) were added to the substrate, but no color change was observed. Upon the addition of H_2O_2, the supernatant's color clearly changed to green, exhibiting a high absorption strength at 417 nm, which is indicative of oxidized ABTS. Our findings suggest that BSA-Cu NFs are laccase mimics rather than other oxidases that generate H_2O_2. The BSA-Cu-NFs induced the oxidation of other phenols, such as catechol, dopamine, and hydroquinone, as shown by color change from the reaction with 4-aminoantipyrine (4-AP) (Fig. S11c). Notably, the BSA-Cu NFs showed much higher activities with all employed phenolic substrates than natural laccase.

Kinetic analyses of BSA-Cu NFs and natural laccase were subsequently performed using epinephrine as a substrate. Using the Michaelis–Menten curves and corresponding Lineweaver–Burk plots, kinetic parameters (K_m, V_{max}, and k_{cat}) were calculated (Fig. S9b, c, and Table S2). Importantly, the K_m of BSA-Cu NFs was ~20 % smaller than that of natural laccase, proving their higher affinity for epinephrine, presumably due to the higher amount of Cu in BSA-Cu NFs (7.64 % calculated from EDS analysis) than that in laccase (~0.32 %) [54]. The k_{cat} values of BSA-Cu NFs were ~7 order higher than that of laccase due to their abundant Cu-based active sites in each NF particle. In addition, SA value of BSA-Cu NFs toward epinephrine oxidation was calculated as 1.63 U/mg, suggesting their effective catalytic performance (Fig. S10c, d).

A high stability against diverse environments is crucial to realize practical enzymatic applications. To evaluate this, peroxidase-laccase dual-enzymatic BSA-Cu NFs and their natural enzyme counterparts (HRP and laccase) were incubated over various pH (2–12) and temperature (4–80 °C) conditions for 3 h, and the remaining activities were assessed. Notably, under all employed conditions, BSA-Cu NFs were

found to retain >90 % of their peroxidase- and laccase-like activities (Fig. S12a, b). However, both HRP and laccase lost most of their activities under acidic and basic pH conditions (≤pH 3 and ≥ pH 11) or high temperature conditions over 50 °C. BSA-Cu NFs also exhibited excellent long-term storage stability, retaining over 90 % of their initial catalytic activity after 15 days at RT, whereas HRP and laccase lost most of their activity after approximately 7 and 9 days, respectively (Fig. S12c). The remarkable robustness of BSA-Cu NFs can be attributed to their hybrid organic-inorganic nanostructures, where proteins were embedded within rigid metal phosphate matrix. This immobilization significantly reduces conformational flexibility and shields the protein from external stimuli, thereby minimizing its susceptibility to denaturation and preserving its catalytic functionality. In addition, their reusability was confirmed through five consecutive cycles, during which the nanoflowers maintained over 90 % of their original activity (Fig. S13). These results confirmed that while natural enzymes under extreme conditions are fragile, the same conditions had no remarkable effects on the activities of BSA-Cu NFs, which is beneficial for real-world applications.

3.3. Colorimetric detection of ascorbic acid and degradation of phenolic dyes based on the peroxidase-laccase dual-enzymatic activities of BSA-Cu NFs

Because abnormal physiological levels of ascorbic acid are closely associated with several chronic diseases such as scurvy, atherosclerosis, cataract, and cancer [2], its simple, rapid, and sensitive detection is important. Here, the peroxidase-like activity of BSA-Cu NFs was exploited to colorimetrically detect ascorbic acid levels. In the assay, peroxidase-like BSA-Cu NFs induced the oxidation of TMB to produce a blue color in the presence of H_2O_2. To the solution, a sample solution containing the target ascorbic acid was added to obtain rapid reduction of oxidized blue TMB to colorless TMB by the antioxidant action of ascorbic acid, which might be derived from its phenolic hydroxy groups to facilitate electron transfer for reducing the oxidized TMB.

The sensing system selectively detected the target ascorbic acid based on the vivid reduction in the blue color intensity, while other interfering molecules, such as carbohydrates (glucose, fructose, lactose), ions (Ca^{2+}, Na^{+}), amino acids (glycine, histidine), and protein (BSA), still showed deep blue color even at 10–fold higher concentrations (Fig. 4a). As the concentration of ascorbic acid was increased to 1 mM, the respective absorption intensity at 652 nm decreased accordingly (Fig. 4b). From the calibration plot, the linear range was measured to be 1–60 μM with the following equation: $y = 0.0127x - 0.0123$ ($R^2 = 0.9981$). The LOD was as low as 0.15 μM. As shown in Table S3, the sensitivity of the BSA-Cu NF-mediated colorimetric assay ranked among the highest compared with those of recently reported ascorbic acid biosensors using diverse nanomaterials.

The practical applicability of the BSA-Cu NF-mediated colorimetric assay was verified by quantitatively determining the ascorbic acid levels in spiked human serum samples. The original concentration of ascorbic acid within 10-fold diluted human serum was measured to be 6.35 μM using an ascorbic acid assay kit, consistent with recent reports [55,56]. After spiking with five representative concentrations (10, 15, 20, 30, and 40 μM), the combined levels were precisely and accurately determined, yielding coefficients of variation (CV) in the range of 0.76 to 3.39 % and recoveries of 96.2–100.8 % (Table 1). These results demonstrate that the developed BSA-Cu NF-mediated colorimetric assay could be a promising method for the convenient determination of ascorbic acid in real clinical samples.

The laccase-like catalytic activity of BSA-Cu NFs was harnessed for the degradation of phenolic dyes, a process where natural laccase is conventionally utilized [57–59]. To evaluate their degradation performance, BSA-Cu NFs were tested against CV, NR, and RB, with free laccase serving as a reference. Following a 2-day incubation at RT, BSA-Cu NFs achieved over 80 % decolorization and breakdown of the dyes, significantly outperforming natural laccase, which exhibited less than 30 % degradation under identical conditions (Fig. 5). The dye removal efficiency of BSA-Cu NFs was strongly influenced by pH and

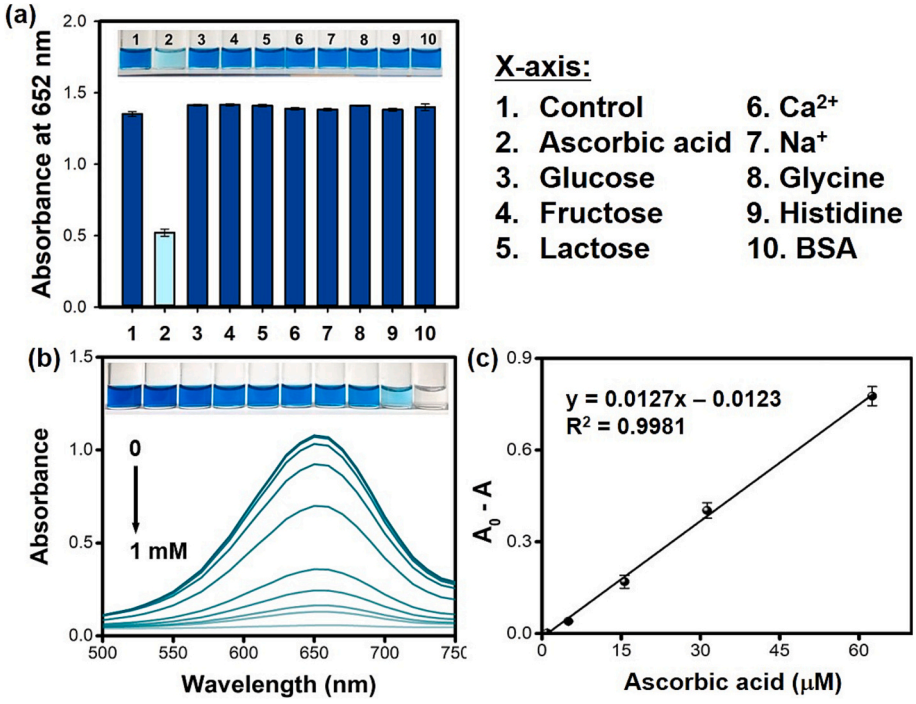

Fig. 4. Colorimetric detection of ascorbic acid based on the peroxidase-like activity of BSA-Cu NFs. (a) Selectivity for detecting ascorbic acid (0.1 mM) among interfering molecules (1 mM). (b) Absorption spectra of BSA-Cu NFs for detecting ascorbic acid at various levels from 0 to 1 mM and their (c) linear calibration plots. In the assay, the reaction mixture containing TMB (0.5 mM), BSA-Cu NFs (0.05 mg/mL), and H_2O_2 (10 mM) in sodium acetate buffer (100 μL, 50 mM, pH 4) was incubated at RT for 15 min. Subsequently, the sample solution (100 μL) containing ascorbic acid was added into the blue-colored mixture, and after 1 min, the reduction in absorbance at 652 nm was recorded.

Table 1
Detection precision of the BSA-Cu NF-based assay for quantitatively determining ascorbic acid levels spiked in human serum samples.

Found in human serum[a] (μM)	Added (μM)	Expected (μM)	Measured[b] (μM)	Recovery[c] (%)	SD[d]	CV[e] (%)
6.35	10	16.35	15.72	96.15	0.36	2.29
	15	21.35	21.52	100.79	0.44	2.03
	20	26.35	25.65	97.34	0.87	3.39
	30	36.35	36.12	99.36	0.78	2.15
	40	46.35	46.02	99.29	0.35	0.76

[a] 10-fold dilution.
[b] Average value of five measurements.
[c] Recovery = (Measured value / Expected value) × 100.
[d] SD (standard deviation) of five measurements.
[e] CV (coefficient of variation) = (SD / average) × 100.

temperature, with optimal performance observed at pH 6–8 and RT (Fig. S14). These pH conditions align with typical environmental water parameters, highlighting the system's practicality for real-world applications. Although slightly enhanced performance was noted at elevated temperatures, RT was selected as the optimal condition due to its operational simplicity and energy efficiency. This pronounced catalytic efficiency highlights the potential of BSA-Cu NFs as robust and multifunctional agents for environmental remediation, particularly in the treatment of phenolic pollutants.

4. Conclusions

Among the BSA-metal hybrid NFs incorporating six different cationic ions (Cu^{2+}, Mn^{2+}, Zn^{2+}, Fe^{2+}, Co^{2+}, and Ca^{2+}) as inorganic constituents, BSA-Cu NFs were found to exhibit the best flower-like morphology as well as unique peroxidase–laccase dual-enzymatic activities, which can be attributed to the Cu coordinated with BSA within the NF matrices with a porous and large surface area. Based on the peroxidase-like

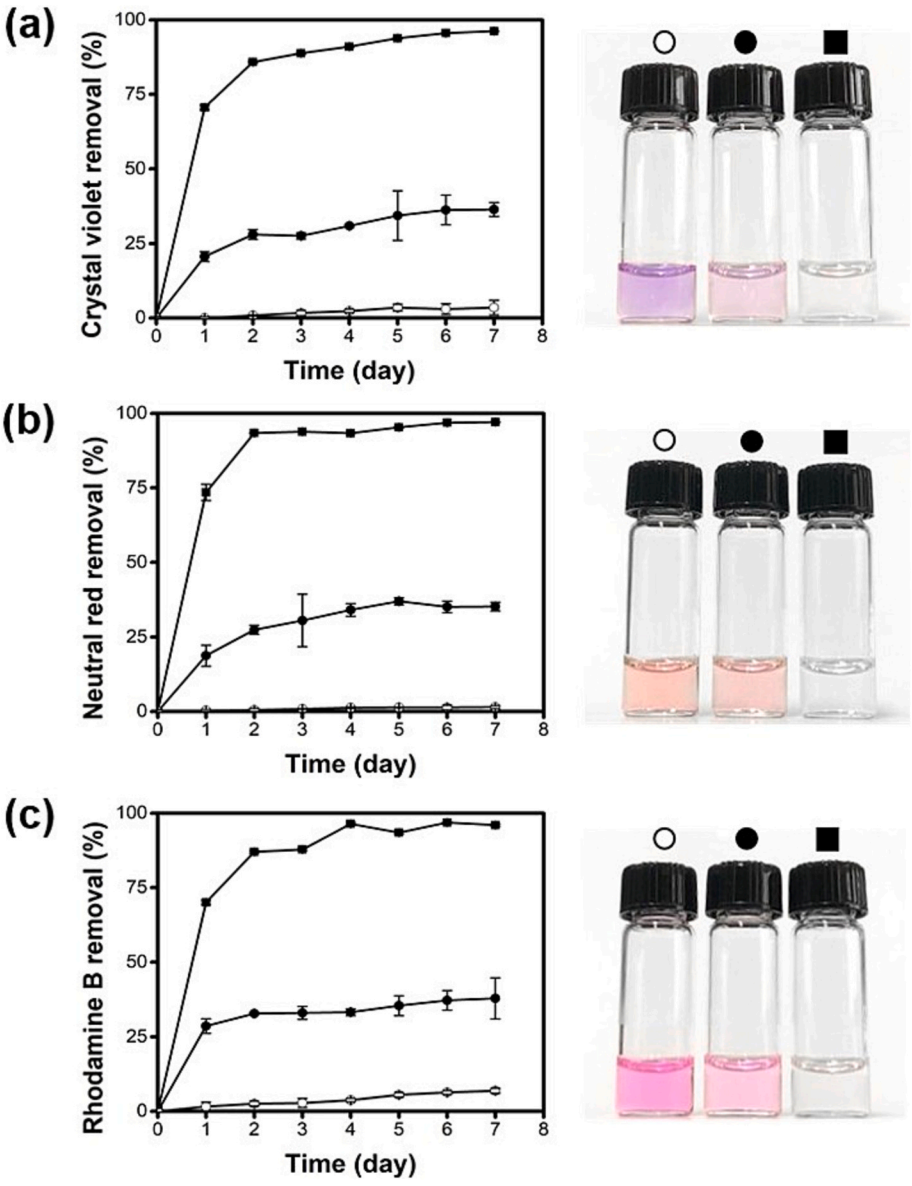

Fig. 5. Degradation efficiencies of (a) crystal violet (CV), (b) neutral red (NR), and (c) rhodamine B (RB) by laccase-like BSA-Cu NFs and natural laccase with the corresponding photographs (○: control, ●: natural laccase, ■: BSA-Cu NFs). The images show the real color of the phenolic dyes (CV, NR, and RB) after treatment for 7 days. In the experiment, BSA-Cu NFs or natural laccase (1 mg/mL) were incubated with a dye solution (CV: 2.5 mg/L, NR: 7.5 mg/L, RB: 1.5 mg/L) at RT in the dark. Degradation was monitored by measuring the absorbance at 590 nm, 523 nm, and 543 nm, respectively.

activity of BSA-Cu NFs, ascorbic acid was colorimetrically detected by its antioxidant action, achieving a remarkable LOD and high precision for detecting ascorbic acid in human serum. Several phenolic dyes were also efficiently degraded by the laccase-like activity of BSA-Cu NFs, at a much faster rate than that by natural laccase. Notably, BSA-Cu NFs offered several advantages: simple and mild synthesis conditions, dual enzymatic functionality, excellent structural and catalytic stability over a wide pH and temperature range, and strong applicability in both biosensing and environmental remediation. Collectively, these findings position BSA-Cu NFs as a promising class of multifunctional biomimetic catalysts with the potential to substitute natural enzymes in diverse practical applications. Nonetheless, challenges such as relatively lower substrate specificity and the need for further optimization to balance dual enzymatic performance warrant future investigation.

CRediT authorship contribution statement

Xuan Ai Le: Writing – original draft, Investigation, Conceptualization. **Thinh Viet Dang:** Validation, Methodology, Investigation. **Moon Il Kim:** Writing – review & editing, Supervision, Conceptualization.

Declaration of competing interest

The authors declare that they have no known competing financial interests or personal relationships that could have appeared to influence the work reported in this paper.

Acknowledgements

This work was supported by a National Research Foundation of Korea (NRF) grant funded by the Korean government (Ministry of Science and ICT [RS-2023-NR077205]) and by the Gachon University research fund of 2024 (GCU-202403870001).

Appendix A. Supplementary data

Supplementary data to this article can be found online at https://doi.org/10.1016/j.ijbiomac.2025.146912.

Data availability

Data will be made available on request.

References

[1] N. Wu, Y. Pan, Q. Liu, F. Shahidi, H.-Y. Li, F. Chen, Z.-Y. Deng, Z.-H. Zhang, Protective benefits and mechanisms of *Phyllanthus emblica* Linn. on aging induced by oxidative stress: a system review, Food Med. Homology 2 (2) (2025), https://doi.org/10.26599/FMH.2025.9420029.

[2] A. Ali, S. Riaz, W. Khalid, M. Fatima, U. Mubeen, Q. Babar, M.F. Manzoor, M. Zubair Khalid, F.K. Madilo, Potential of ascorbic acid in human health against different diseases: an updated narrative review, Int. J. Food Prop. 27 (1) (2024) 493–515, https://doi.org/10.1080/10942912.2024.2327335.

[3] J. Lin, W. Ye, M. Xie, D.H. Seo, J. Luo, Y. Wan, B. Van der Bruggen, Environmental impacts and remediation of dye-containing wastewater, Nat. Rev. Earth Environ. 4 (11) (2023) 785–803, https://doi.org/10.1038/s43017-023-00489-8.

[4] Q. Wang, H. Wei, Z. Zhang, E. Wang, S. Dong, Nanozyme: an emerging alternative to natural enzyme for biosensing and immunoassay, TrAC Trends Anal. Chem. 105 (2018) 218–224, https://doi.org/10.1016/j.trac.2018.05.012.

[5] B. Unnikrishnan, C.-W. Lien, H.-W. Chu, C.-C. Huang, A review on metal nanozyme-based sensing of heavy metal ions: challenges and future perspectives, J. Hazard. Mater. 401 (2021) 123397, https://doi.org/10.1016/j.jhazmat.2020.123397.

[6] Q. Tian, S. Li, Z. Tang, Z. Zhang, D. Du, X. Zhang, X. Niu, Y. Lin, Nanozyme-enabled biomedical diagnosis: advances, trends, and challenges, Adv. Healthc. Mater. 14 (2025) e2401630, https://doi.org/10.1002/adhm.202401630.

[7] Y. Zhang, G. Wei, W. Liu, T. Li, Y. Wang, M. Zhou, Y. Liu, X. Wang, H. Wei, Nanozymes for nanohealthcare, Nat. Rev. Methods Primers 4 (2024) 36, https://doi.org/10.1038/s43586-024-00315-5.

[8] X. Yuan, X. He, J. Fan, Y. Tai, Y. Yao, Y. Luo, J. Chen, H. Luo, X. Zhou, F. Lou, Q. Niu, W. Hu, X. Sun, B. Ying, Advances in nanozymes with peroxidase-like activity for biosensing and disease therapy applications, J. Mater. Chem. B 13 (5) (2025) 1599–1618, https://doi.org/10.1039/D4TB02315C.

[9] M. Feng, X. Li, X. Zhang, Y. Huang, Recent advances in the development and analytical applications of oxidase-like nanozymes, TrAC Trends Anal. Chem. 166 (2023) 117220, https://doi.org/10.1016/j.trac.2023.117220.

[10] D. Xu, L. Wu, H. Yao, L. Zhao, Catalase-like nanozymes: classification, catalytic mechanisms, and their applications, Small 18 (37) (2022) 2203400, https://doi.org/10.1002/smll.202203400.

[11] H. Zhao, R. Zhang, X. Yan, K. Fan, Superoxide dismutase nanozymes: an emerging star for anti-oxidation, J. Mater. Chem. B 9 (35) (2021) 6939–6957, https://doi.org/10.1039/D1TB00720C.

[12] J. He, J. Li, Y. Wang, Y. Wang, P. Wu, Recent progress on the rational design of laccase mimics, Chem. Asian J. (2025) e202401942, https://doi.org/10.1002/asia.202401942.

[13] L. Wang, B. Wang, K. Kang, X. Ji, Y. Niu, C. Li, Y. Wang, Defect-engineered porous carbon stabilizes Pt-N4 sites for enhanced laccase-like activity: a nanozyme sensor for sensitive detection of luteolin, Microchem. J. (2025) 114182, https://doi.org/10.1016/j.microc.2025.114182.

[14] H. Yin, Y. Tian, Z. Liang, C. Cao, F. Wang, Z. Qiao, D. Wei, N. Zhu, Z. Zhang, Laccase activity regulation of platinum-based nanozymes by support engineering strategy and application in heavy metal ions sensing, Microchem. J. (2025) 113947, https://doi.org/10.1016/j.microc.2025.113947.

[15] J. Sheng, Y. Wu, H. Ding, K. Feng, Y. Shen, Y. Zhang, N. Gu, Multienzyme-like nanozymes: regulation, rational design, and application, Adv. Mater. 36 (2024) e2211210, https://doi.org/10.1002/adma.202211210.

[16] X. Zhu, N. Xu, L. Zhang, D. Wang, P. Zhang, Novel design of multifunctional nanozymes based on tumor microenvironment for diagnosis and therapy, Eur. J. Med. Chem. 238 (2022) 114456, https://doi.org/10.1016/j.ejmech.2022.114456.

[17] D. Li, D. Dai, G. Xiong, S. Lan, C. Zhang, Metal-based nanozymes with multienzyme-like activities as therapeutic candidates: applications, mechanisms, and optimization strategy, Small 19 (2023) e2205870, https://doi.org/10.1002/smll.202205870.

[18] J. Cui, S. Jia, Organic-inorganic hybrid nanoflowers: a novel host platform for immobilizing biomolecules, Coord. Chem. Rev. 352 (2017) 249–263, https://doi.org/10.1016/j.ccr.2017.09.008.

[19] M. Zhang, Y. Zhang, C. Yang, C. Ma, J. Tang, Enzyme-inorganic hybrid nanoflowers: classification, synthesis, functionalization and potential applications, Chem. Eng. J. 415 (2021) 129075, https://doi.org/10.1016/j.cej.2021.129075.

[20] A.A. Caparco, D.R. Dautel, J.A. Champion, Protein mediated enzyme immobilization, Small 18 (19) (2022) 2106425, https://doi.org/10.1002/smll.202106425.

[21] H. Jafari-Nodoushan, S. Mojtabavi, M.A. Faramarzi, N. Samadi, Organic-inorganic hybrid nanoflowers: the known, the unknown, and the future, Adv. Colloid Interf. Sci. 309 (2022) 102780, https://doi.org/10.1016/j.cis.2022.102780.

[22] J. Chen, Z. Guo, Y. Xin, Z. Gu, L. Zhang, X.J.C.C.R. Guo, Organic-inorganic hybrid nanoflowers: a comprehensive review of current trends, advances, and future perspectives, Coord. Chem. Rev. 489 (2023) 215191, https://doi.org/10.1016/j.ccr.2023.215191.

[23] I.G. Subramani, V. Perumal, S.C.B. Gopinath, K.S. Fhan, N.M. Mohamed, Organic-inorganic hybrid nanoflower production and analytical utilization: fundamental to cutting-edge technologies, Crit. Rev. Anal. Chem. 52 (2022) 1488–1510, https://doi.org/10.1080/10408347.2021.1889962.

[24] K. Xu, B. Appiah, B.-W. Zhang, Z.-H. Yang, C. Quan, Recent advances in enzyme immobilization based on nanoflowers, J. Catal. 418 (2023) 31–39, https://doi.org/10.1016/j.jcat.2023.01.001.

[25] E. Gokturk, I. Ocsoy, E. Turac, E. Sahmetlioglu, Horseradish peroxidase-based hybrid nanoflowers with enhanced catalytical activities for polymerization reactions of phenol derivatives, Polym. Adv. Technol. 31 (2020) 2371–2377, https://doi.org/10.1002/pat.4956.

[26] S.K.S. Patel, R.K. Gupta, I.-W. Kim, J.-K. Lee, Coriolus versicolor laccase-based inorganic protein hybrid synthesis for application in biomass saccharification to enhance biological production of hydrogen and ethanol, Enzym. Microb. Technol. 170 (2023) 110301, https://doi.org/10.1016/j.enzmictec.2023.110301.

[27] D. Kim, B.C. Kim, E.T. Hwang, Double crystallization-driven copper-2-methylimidazole nanoflowers: stabilizing glucose oxidase and activating nanozyme functions for tandem catalysis, Int. J. Biol. Macromol. 315 (2025) 144341, https://doi.org/10.1016/j.ijbiomac.2025.144341.

[28] K.W. Kim, D. Kim, B.C. Kim, E.T. Hwang, Development of cross-linked glucose oxidase integrated Cu-nanoflower electrode for reusable and stable glucose sensing, Int. J. Biol. Macromol. 275 (2024) 133605, https://doi.org/10.1016/j.ijbiomac.2024.133605.

[29] N. Özdemir, C. Altinkaynak, M. Türk, F. Geçili, S. Tavlaşoğlu, Amino acid-metal phosphate hybrid nanoflowers (AaHNFs): their preparation, characterization and anti-oxidant capacities, Polym. Bull. 79 (11) (2022) 9697–9716, https://doi.org/10.1007/s00289-021-03973-7.

[30] X. Zheng, Q. Lian, L. Zhou, Y. Jiang, J. Gao, Peroxidase mimicking of binary polyacrylonitrile-CuO nanoflowers and the application in colorimetric detection of H_2O_2 and ascorbic acid, ACS Sustain. Chem. Eng. 9 (20) (2021) 7030–7043, https://doi.org/10.1021/acssuschemeng.1c00723.

[31] T.N. Le, X.A. Le, T.D. Tran, K.J. Lee, M.I. Kim, Laccase-mimicking Mn–Cu hybrid nanoflowers for paper-based visual detection of phenolic neurotransmitters and rapid degradation of dyes, J. Nanobiotechnol. 20 (1) (2022) 358, https://doi.org/10.1186/s12951-022-01560-0.

[32] J. Ge, J. Lei, R.N. Zare, Protein–inorganic hybrid nanoflowers, Nat. Nanotechnol. 7 (2012) 428–432, https://doi.org/10.1038/nnano.2012.80.

[33] L. Gao, J. Zhuang, L. Nie, J. Zhang, Y. Zhang, N. Gu, T. Wang, J. Feng, D. Yang, S. Perrett, X. Yan, Intrinsic peroxidase-like activity of ferromagnetic nanoparticles, Nat. Nanotechnol. 2 (2007) 577–583, https://doi.org/10.1038/nnano.2007.260.
[34] S. Behera, P. Mohanty, P.P. Dash, P. Mohapatra, L. Shubhadarshinee, R. Behura, A. K. Barick, P. Mohapatra, B.R. Jali, Selective binding of bovine serum albumin (BSA): a comprehensive review, Biointerface Res. Appl. Chem. 13 (2023) 555, https://doi.org/10.33263/BRIAC136.555.
[35] T. Topală, A. Bodoki, L. Oprean, R. Oprean, Bovine serum albumin interactions with metal complexes, Clujul Med. 87 (4) (2014) 215, https://doi.org/10.15386/cjmed-357.
[36] C. Liu, J. Zheng, B. Zhang, X. Zhong, W. Wang, Z. Li, BSA-$Cu_3(PO_4)_2$ hybrid nanoflower—an efficient and low-cost nanoenzyme for decolorization of organic pollutants, Anal. Bioanal. Chem. 415 (2023) 1687–1698, https://doi.org/10.1007/s00216-023-04563-4.
[37] T. Su, J. Lu, R. Thomas, Z. Cui, J. Penfold, The conformational structure of bovine serum albumin layers adsorbed at the silica− water Interface, J. Phys. Chem. B 102 (41) (1998) 8100–8108, https://doi.org/10.1021/jp981239t.
[38] L.R. Barbosa, M.G. Ortore, F. Spinozzi, P. Mariani, S. Bernstorff, R. Itri, The importance of protein-protein interactions on the pH-induced conformational changes of bovine serum albumin: a small-angle X-ray scattering study, Biophys. J. 98 (1) (2010) 147–157.
[39] N. Fang, Y.-M. Ji, C.-Y. Li, Y.-Y. Wu, C.-G. Ma, H.-L. Liu, M.-X. Li, Synthesis and adsorption properties of [Cu (L) 2 (H 2 O)] H 2 [Cu (L) 2 (P 2 Mo 5 O 23)]·4H 2 O/Fe 3 O 4 nanocomposites, RSC Adv. 7 (41) (2017) 25325–25333, https://doi.org/10.1039/C7RA02133J.
[40] C. Ji, J. Zheng, Y. Jin, X.b. Yin, S. Han, M. Zhang, In site generation of well-dispersed Ag3PO4 NPs on protein-inorganic hybrid nanoflowers with enhanced catalytic performance, Chemistryselect 7 (10) (2022) e202104143, https://doi.org/10.1002/slct.202104143.
[41] Z. Wang, P. Liu, Z. Fang, H. Jiang, Trypsin/$Zn_3(PO_4)_2$ hybrid nanoflowers: controlled synthesis and excellent performance as an immobilized enzyme, Int. J. Mol. Sci. 23 (2022) 11853, https://doi.org/10.3390/ijms231911853.
[42] T.V. Dang, J.M. Kim, M.I. Kim, Ficin-copper hybrid nanoflowers with enhanced peroxidase-like activity for colorimetric detection of biothiols, Mikrochim. Acta 190 (2023) 473, https://doi.org/10.1007/s00604-023-06070-w.
[43] J. Wu, X. Ma, C. Li, X. Zhou, J. Han, L. Wang, H. Dong, Y. Wang, A novel photon-enzyme cascade catalysis system based on hybrid HRP-CN/$Cu_3(PO_4)_2$ nanoflowers for degradation of BPA in water, Chem. Eng. J. 427 (2022) 131808, https://doi.org/10.1016/j.cej.2021.131808.
[44] T.V. Dang, N.S. Heo, H.-J. Cho, S.M. Lee, M.Y. Song, H.J. Kim, M.I. Kim, Colorimetric determination of phenolic compounds using peroxidase mimics based on biomolecule-free hybrid nanoflowers consisting of graphitic carbon nitride and copper, Mikrochim. Acta 188 (2021) 293, https://doi.org/10.1007/s00604-021-04937-4.
[45] J.H. Choi, J.W. Kang, H.Y. Koo, Y.C. Kang, Lithiophilic and conductive CuO-Cu2O-cu microspheres with controlled void structure via spray pyrolysis for improved lithium metal anode performance, Int. J. Energy Res. 2023 (2023) 2200257, https://doi.org/10.1155/2023/2200257.
[46] S. Ravi, S. Zhang, Y.-R. Lee, K.-K. Kang, J.-M. Kim, J.-W. Ahn, W.-S. Ahn, EDTA-functionalized KCC-1 and KIT-6 mesoporous silicas for Nd3+ ion recovery from aqueous solutions, J. Ind. Eng. Chem. 67 (2018) 210–218, https://doi.org/10.1016/j.jiec.2018.06.031.
[47] T. Wang, R. Yang, N. Shi, J. Yang, H. Yan, J. Wang, Z. Ding, W. Huang, Q. Luo, Y. Lin, Cu, N-codoped carbon nanodisks with biomimic stomata-like interconnected hierarchical porous topology as efficient electrocatalyst for oxygen reduction reaction, Small 15 (43) (2019) 1902410, https://doi.org/10.1002/smll.201902410.
[49] B. Jiang, D. Duan, L. Gao, M. Zhou, K. Fan, Y. Tang, J. Xi, Y. Bi, Z. Tong, G.F. Gao, Standardized assays for determining the catalytic activity and kinetics of peroxidase-like nanozymes, Nat. Protoc. 13 (7) (2018) 1506–1520, https://doi.org/10.1038/s41596-018-0001-1.
[50] C. Zhao, C. Xiong, X. Liu, M. Qiao, Z. Li, T. Yuan, J. Wang, Y. Qu, X. Wang, F. Zhou, Unraveling the enzyme-like activity of heterogeneous single atom catalyst, Chem. Commun. 55 (16) (2019) 2285–2288, https://doi.org/10.1039/C9CC00199A.
[51] T.D. Tran, P.T. Nguyen, T.N. Le, M.I. Kim, DNA-copper hybrid nanoflowers as efficient laccase mimics for colorimetric detection of phenolic compounds in paper microfluidic devices, Biosens. Bioelectron. 182 (2021) 113187, https://doi.org/10.1016/j.bios.2021.113187.
[52] P.T. Nguyen, T.H. Vu, M.I. Kim, Histidine–cysteine–copper hybrid nanoflowers as active site-inspired laccase mimics for the colorimetric detection of phenolic compounds in PDMS microfluidic devices, Sensors Actuators B Chem. 413 (2024) 135845, https://doi.org/10.1016/j.snb.2024.135845.
[53] J. Wang, R. Huang, W. Qi, R. Su, B.P. Binks, Z. He, Construction of a bioinspired laccase-mimicking nanozyme for the degradation and detection of phenolic pollutants, Appl. Catal. B 254 (2019) 452–462, https://doi.org/10.1016/j.apcatb.2019.05.012.
[54] H. Liang, F. Lin, Z. Zhang, B. Liu, S. Jiang, Q. Yuan, J. Liu, Multicopper laccase mimicking nanozymes with nucleotides as ligands, ACS Appl. Mater. Interfaces 9 (2017) 1352–1360, https://doi.org/10.1021/acsami.6b15124.
[55] J. Zheng, D. Song, H. Chen, J. Xu, N.S. Alharbi, T. Hayat, M. Zhang, Enhanced peroxidase-like activity of hierarchical MoS_2-decorated N-doped carbon nanotubes with synergetic effect for colorimetric detection of H_2O_2 and ascorbic acid, Chin. Chem. Lett. 31 (2020) 1109–1113, https://doi.org/10.1016/j.cclet.2019.09.037.
[56] Y. Cen, J. Tang, X.-J. Kong, S. Wu, J. Yuan, R.-Q. Yu, X. Chu, A cobalt oxyhydroxide-modified upconversion nanosystem for sensitive fluorescence sensing of ascorbic acid in human plasma, Nanoscale 7 (2015) 13951–13957, https://doi.org/10.1039/C5NR03588K.
[57] J. Jeyabalan, A. Veluchamy, V.P. V, A. Kumar, R. Chandrasekar, S. Narayanasamy, A review on the laccase assisted decolourization of dyes: recent trends and research progress, J. Taiwan Inst. Chem. Eng. 151 (2023) 105081, https://doi.org/10.1016/j.jtice.2023.105081.
[58] S. Naseem, R.S. Rawal, D. Pandey, S.K. Suman, Immobilized laccase: an effective biocatalyst for industrial dye degradation from wastewater, Environ. Sci. Pollut. Res. Int. 30 (2023) 84898–84917, https://doi.org/10.1007/s11356-023-28275-5.
[59] Z. Chen, W.-D. Oh, P.-S. Yap, Recent advances in the utilization of immobilized laccase for the degradation of phenolic compounds in aqueous solutions: a review, Chemosphere 307 (Pt 3) (2022) 135824, https://doi.org/10.1016/j.chemosphere.2022.135824.